Bryn Mawr College
Scholarship, Research, and Creative Work at Bryn Mawr College

Physics Faculty Research and Scholarship | Physics

2003

Back and Forth Between Rydberg Atoms and Ultracold Plasmas

T. F. Gallagher

P. Pillet

M. P. Robinson

B. Laburthe-Tolra

Michael Noel
Bryn Mawr College, mnoel@brynmawr.edu

Let us know how access to this document benefits you.

Follow this and additional works at: http://repository.brynmawr.edu/physics_pubs

 Part of the Physics Commons

Custom Citation
T.F. Gallagher *et al.*, *J. Opt. Soc. Am. B* **20**, 1091 (2003).

This paper is posted at Scholarship, Research, and Creative Work at Bryn Mawr College. http://repository.brynmawr.edu/physics_pubs/32

For more information, please contact repository@brynmawr.edu.

Back and forth between Rydberg atoms and ultracold plasmas

T. F. Gallagher

Department of Physics, University of Virginia, Charlottesville, Virginia 22904-4714, and Laboratoire Aime Cottón, Batiment 505, Centre National de la Recherche Scientifique II, Campus d'Orsay, 91405 Orsay Cedex, France

P. Pillet, M. P. Robinson, and B. Laburthe-Tolra

Laboratoire Aime Cottón, Batiment 505, Centre National de la Recherche Scientifique II, Campus d'Orsay, 91405 Orsay Cedex, France

Michael W. Noel

Department of Physics, University of Virginia, Charlottesville, Virginia 22904-4714, and Department of Physics, Bryn Mawr College, Bryn Mawr, Pennsylvania 19010

Received August 1, 2002; revised manuscript received November 19, 2002

By photoionizing cold, trapped atoms it is possible to produce ultracold plasmas with temperatures in the vicinity of 1 K, roughly 4 orders of magnitude colder than conventional cold plasmas. After the first photoelectrons leave, the resulting positive charge traps the remaining electrons in the plasma. Monitoring the dynamics of the expansion of these plasmas shows explicitly the flow of energy from electrons to the ionic motion, which is manifested as the expansion of the plasma. The electron energy can either be their initial energy from photoionization or can come from the energy redistribution inherent in recombination and superelastic scattering from recombined Rydberg atoms. If the cold atoms are excited to Rydberg states instead of being photoionized, the resulting cold Rydberg gas quickly evolves into an ultracold plasma. After a few percent of the atoms are ionized by collisions or blackbody radiation, electrons are trapped by the resulting positive charge, and they quickly lead to ionization of the Rydberg atoms, forming a plasma. While the source of this energy is not clear, a likely candidate is superelastic scattering, also thought to be important for the expansion of deliberately made plasmas. © 2003 Optical Society of America

OCIS codes: 020.2070, 020.5780, 020.7010.

1. INTRODUCTION

The conventional definition of a plasma is an ionized gas that is macroscopically neutral and has a Debye length, λ_D, that is smaller than the size of the sample.[1] The Debye length is defined as

$$\lambda_D = \left(\frac{2\epsilon_0 kT}{Ne^2}\right)^{1/2}, \tag{1}$$

where ϵ_0 is the permittivity of free space, k is the Boltzmann constant, T is the temperature, e is the electron charge, and N is the ion and electron density, assumed to be equal. From Eq. (1) it is straightforward to show that two charged particles separated by a Debye length have a Coulomb interaction energy comparable with their kinetic energy kT. If two charged particles are separated by a distance that is large compared with the Debye length, the intervening particles move so as to screen the potential that is due to one and seen by the other, and the potential from a charged particle at a distance r is given by

$$V = -\frac{1}{r}\exp(-r/\lambda_D). \tag{2}$$

Here and hereafter we use atomic units, unless units are explicitly given. If λ_D is larger than the sample the charged particles all behave as individual particles. On the other hand, if λ_D is smaller than the sample size, much of the volume experiences the screening of Eq. (2), and the sample exhibits the collective properties of a plasma.

Until recently a cold plasma was one with a temperature of ~10 000 K. While this does not seem particularly cold, it is easy to see that this is nearly the minimum possible temperature at which a plasma can sustain itself through ionizing collisions of the electrons with neutral gas atoms. The lowest ionization potentials of atoms are ~5 eV, which is the lowest possible energy an electron can have to ionize the atom. To have a reasonable fraction (1%) of the electrons with energies in excess of 5 eV requires that $kT \sim 1$ eV, or $T \approx 10\,000$ K.

The possibility of cold trapped atoms and ions has completely changed our notion of what a cold plasma can be. Elegant experiments have been done with one-component plasmas formed by cold ions in traps.[2] The trap fields replace the electrons in a normal plasma. It has been possible to observe the crystallization of the ions and explore many properties analogous to those seen in ionic solids.

Cold trapped neutral atoms have made it possible to produce neutral—or very nearly so—ultracold plasmas. In this paper we briefly review this work and the closely

 © 2003 Optical Society of America

related work with ultracold Rydberg gases, which can spontaneously evolve into an ultracold plasma.

2. ULTRACOLD PLASMAS

A beautiful set of experiments conducted at the National Institute for Standards and Technology (NIST) has shown the way into this fascinating area.[3–5] The essential notion of the experiment is to start with cold (30 μK) Xe atoms in a magneto-optical trap (MOT). Typically 10^6 Xe atoms are contained in a trap volume of 0.1 mm^3. The thermal velocity of the Xe atoms is 10 cm/s, so in 1 μs they move a negligible distance compared with the trap dimension. The Xe atoms are photoionized with a pulsed green dye laser tuned just above the ionization limit, resulting in cold ions (30 μK) and electrons whose energy is determined by the tuning of the laser. The photoelectron energy can be <1 cm^{-1} (1 cm^{-1} corresponds to $T = 1.5$ K). The electrons initially all have one energy but come into thermal equilibrium in tens of nanoseconds, producing a very cold plasma. The ions are automatically cold, and tuning the laser sets the electron temperature to the desired value.

The trapped Xe atoms are between two metal grids to which voltages are applied to detect the electrons produced with a particle multiplier. Each time the dye laser fires, the following timing sequence occurs: During and after the 10-ns dye laser pulse there is a constant 5-mV/cm field. After 1.6 μs a slowly rising field ramp is applied as shown in Fig. 1. The result of a typical experiment is shown in Fig. 1, obtained with the dye laser tuned 0.4 cm^{-1} (0.6 K) above the ionization limit. When a small number of photoelectrons are created they are detected promptly at $\sim$1 μs, as shown in the upper trace. As the laser intensity is increased the number of photoelectrons also increases, but a second signal appears later in time, after the onset of the field ramp. Further increases in the laser intensity slightly increase the number of prompt photoelectrons but substantially increase the later signal, until at the highest laser intensity it is the dominant signal.

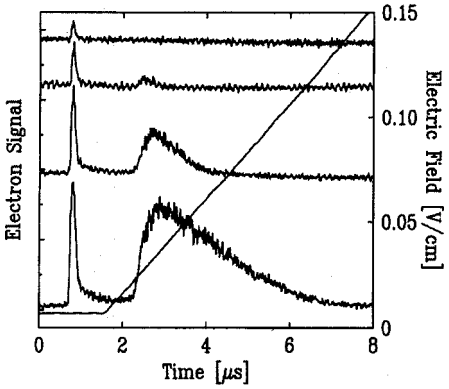

Fig. 1. Electron signals for four different dye-laser pulse energies, which produced charged-particle densities from 10^5–10^7 cm^{-3}. The laser fires at $t = 0$, and the initial kinetic energy of the photoelectrons is 0.4 cm^{-1}. Also shown is the field ramp applied 1.6 μs after the laser pulse. The signal at 1 μs is the prompt photoelectron signal, and the signal after 2 μs is from the plasma (from Ref. 3).

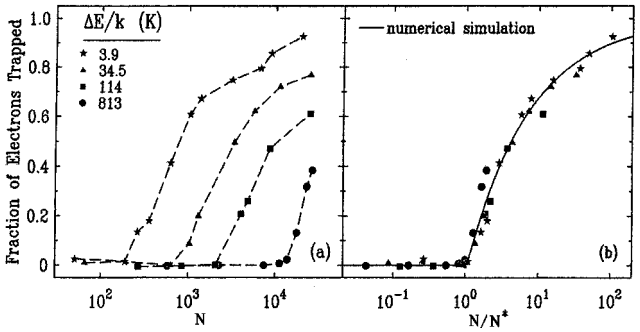

Fig. 2. (a) Fraction of electrons trapped versus number of photons created for different initial photoelectron energies, given in Kelvin. (b) Scaled plot using N/N^+ for all photoelectron energies (from Ref. 3).

The late signal occurs when a plasma has been formed, and why it is late is easily understood by considering what happens over the course of an intense laser pulse. The first photoelectrons produced promptly leave the sample, leading to the prompt signal. Photoelectrons formed later in the pulse experience the macroscopic positive charge left behind and are trapped by it. It is easy to estimate the number of ions required, N^+, by equating the known photoelectron energy E_e with the Coulomb potential at the trap radius R

$$\frac{N^+e^2}{R} = E_e\,. \tag{3}$$

For an energy $E_e = 100$ cm^{-1}, or $T = 145$ K, and a trap radius of 200 μm we find $N^+ = 1700$. Note that once this number of ions is present all future photoelectrons will be trapped, because the net charge of the trap volume remains N^+. Another important observation is that if we assume that $E_e = kT$, at or near the threshold for trapping the photoelectrons, then $\lambda_D \approx R$, and since there is often a much higher density of electrons than at threshold, $\lambda_D \ll R$, and there is a plasma.

Equation (3) implies that it should be easier to form a plasma if the photoelectron energy is lower, and this expectation is borne out by the experiments, as shown by Fig. 2(a). In fact, all the data can be put on a universal curve, as shown in Fig. 2(b).

The plasma is not neutral, and it eventually disappears through evaporation of the hottest electrons and expansion, which reduces the Coulomb binding force. Although one might naively expect the expansion of the plasma to be driven by the net positive space charge, it is not. Rather, the electron energy drives the expansion of the plasma, as demonstrated by measurements of the density or, equivalently, the size of the plasma. The essential idea of the measurement is to detect the response at the plasma frequency, which is proportional to the electron density. A weak rf field at a frequency between 5 and 40 MHz is applied to the plasma; as the plasma expands and its density decreases, the plasma frequency comes into resonance with the applied rf field, at which point it absorbs energy from the rf field, increasing the rate at which electrons evaporate from the plasma. An example is shown in Fig. 3(a). The peak at 10 μs in the electron signal with the rf field indicates that at that time

the plasma frequency is 5 MHz. As shown by Fig. 3(b), at earlier times the plasma frequency is higher and at later times it is lower, providing a quantitative measure of the expansion of the plasma. The radius of the plasma can be represented by

$$R = \sqrt{R_0^2 + (v_0 t)^2}, \tag{4}$$

where R_0 is the initial plasma radius and v_0 its expansion rate. Physically v_0 corresponds to the average outward velocity of the ions, assumed to be constant. What is interesting is that v_0 depends on the energy of the photoelectrons, as shown by Fig. 4. This implies that the initial photoelectron energy is converted into the energy of expansion of the plasma (i.e., the kinetic energy of the ions moving outward). This conversion occurs as follows: The rapidly moving electrons are bound to the macroscopic positive charge, and each time an electron goes outside the positive cloud it is pulled back by the Coulomb attraction. The reaction force on the positive charge pulls it out to larger radius, and it is by this mechanism that the electron energy is converted to the outward ion motion corresponding to the expansion of the plasma.

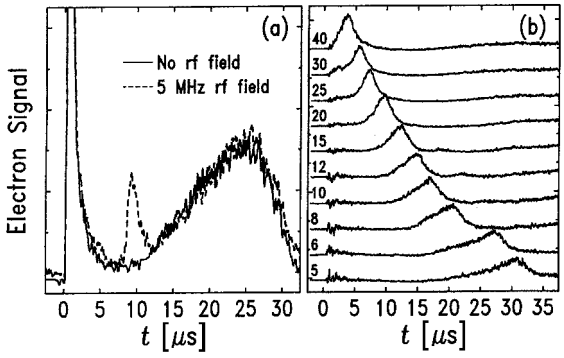

Fig. 3. Electron signals from plasmas created at $t = 0$: (a) 3×10^4 atoms are photoionized with photoelectron initial energy of 360 cm^{-1}, resulting in the plasma signals shown with and without a 5-MHz rf field; (b) electron signals from plasmas initially containing 8×10^4 ions and electrons of 18 cm^{-1} initial energy. In (b) the differences between the traces with and without the rf field are displayed. The plasma response to frequencies from 5–40 MHz is shown in signals that are normalized for clarity. Movement of the plasma response to later times at lower frequencies indicates the expansion of the plasma (from Ref. 4).

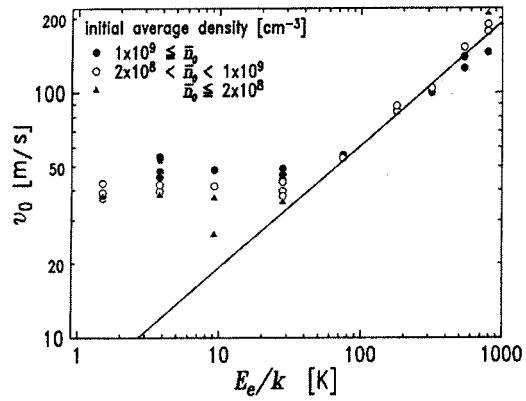

Fig. 4. Expansion velocities of the plasmas versus the initial energy of the photoelectrons E_e, expressed here as a temperature. For $E_C/k_B > 0$ it is clear that the initial electron energy is converted to the expansion of the plasma (from Ref. 4).

The conversion from the initial electron energy to the expansion of the plasma provides a good explanation for the expansion at large photoelectron energies (shown by the right-hand side of Fig. 4), but at low photoelectron energies the observed expansion rates are higher than expected. This puzzle disappeared when field pulses strong enough to ionize Rydberg states were applied to the plasmas. At low photoelectron energies Rydberg states as low as $n = 40$, which is bound by 70 cm^{-1}, were observed; the lower the photoelectron energy, the greater the production of Rydberg atoms. Three-body recombination occurs, i.e., the process

$$e^-(E) + e^-(E) + Xe^+ \rightarrow Xe^*(-E') + e^-(E + E'), \tag{5}$$

and so it leads to higher-energy electrons which in turn lead to more rapid expansion of the plasma, as observed. The rate for three-body recombination scales as $T^{-9/2}$, so it is faster at lower energies. A simple picture of why three-body recombination occurs is provided by molecular dynamics simulations.[6] If in the expansion a three-body collision leaves a slow electron near an ion, then the electron is trapped in a bound state.

While the observation of recombination explains the rapid expansion of the plasma at low photoelectron energy, an aspect of the observations that does not match the usual picture of recombination is that the most deeply bound Rydberg states are observed for the lowest photoelectron energies. As pointed out by Robicheaux and Hanson,[7] one would expect that the binding energy would be similar to the initial energy of the free electrons, i.e., $E' \cong E$ in Eq. (5). They suggest that the deeply bound Rydberg states observed for low photoelectron energies are the result of a two-step process, recombination followed by superelastic collisions. Explicitly, the processes that occur are likely to be

$$e^-(E) + e^-(E) + Xe^+ \rightarrow Xe^*(-E) + e^-(2E), \tag{6}$$

$$e^-(E') + Xe^*(-E) \rightarrow Xe^*(-E - E'') + e^-(E' + E''). \tag{7}$$

In sum, much of the energy transfer to the free electrons comes from the superelastic scattering of Eq. (7). Putting both the processes of Eqs. (6) and (7) into a model leads to a calculated rate of expansion that matches the observed rate of expansion at both high and low photoelectron energies, i.e., over the entire range of Fig. 4.

While all aspects of these ultracold plasmas are not understood, it is clear that their basic properties are well in hand and that it is possible to do experiments with almost perfectly specified initial conditions.

3. EVOLUTION OF COLD RYDBERG ATOMS INTO AN ULTRACOLD PLASMA

While cold Rydberg atoms may seem far removed from plasmas, in fact they are not. For plasma electron and ion densities of 10^{10} cm^{-3} the typical distance from an electron to an ion is 10^{-3} cm, while for an $n = 50$ Ryd-

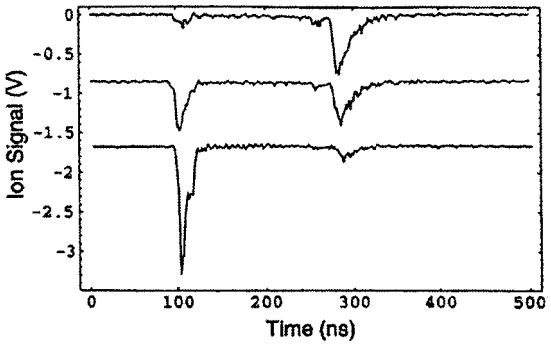

Fig. 5. Oscilloscope traces for three different interaction times showing the evolution of Rb 36*b* atoms at a density of 1.5 $\times$ 10^9 cm^{-3} to a cold plasma. From top to bottom, the traces correspond to a time delay between excitation and field ionization of 2, 5, and 12 μs. In the upper trace there is very little early ion signal and a large late Rydberg atom signal, while the reverse is true for the lower trace, indicating the formation of a plasma (from Refs. 8 and 11).

berg atom the distance is $\sim 10^{-5}$ cm, only a factor of 100 less. One might thus think of the ultracold plasma as being the continuum limit of a cold Rydberg gas. In fact, the only difference between the NIST plasma experiments and the experiments with cold Rydberg gases is that in the former case the laser is tuned just over the limit, whereas in the latter it is tuned just under the limit. With our present knowledge of the energy transfer processes in ultracold plasmas it is perhaps not surprising that cold Rydberg atoms can spontaneously evolve into a plasma. On the other hand, Rydberg atom samples at these densities of 10^{10} cm^{-3} have been studied for some time, so why has the evolution to a plasma only recently been observed? It is presumably because the atoms were not cold and the ion cloud expanded too rapidly to trap the electrons into a plasma.[8] Dense samples, 10^{12}–10^{13} cm^{-3}, of hot Rydberg atoms do evolve into a plasma,[9] and a plasma can easily be formed with hot atoms if electrons are created directly, by photoionization.[10]

In experiments at the University of Virginia and Laboratoire Aime Cottón, Rb (Cs) atoms in a MOT were excited to Rydberg states of $n > 25$ from the $5p$ ($6p$) state with a pulsed dye laser.[8,11,12] As noted above, the excitation was essentially the same as in the NIST experiments except that Rydberg states just below the limit were excited instead of the continuum just above the limit. A variable time after the laser pulse, an electric field ramp of the appropriate polarity is applied to the Rydberg atoms to field ionize them and drive the resulting ions or electrons to a microchannel plate detector. Rydberg states ionize at an electric field given by[13]

$$E = 1/16n^4, \tag{8}$$

so higher-lying states are ionized earlier in the field ramp, and the temporal dependence of the signal can be used to infer the final Rydberg state distribution. There are useful differences between detection of ions and electrons. If free ions are created by any process, they remain in the MOT volume and are detected at the beginning of the field ramp. In contrast, free electrons simply leave the MOT volume and are not detected. A plasma in which the electrons are bound to the macroscopic positive charge of the plasma behaves in the same way as a very high-Rydberg atom ($n \to \infty$), resulting in an electron signal at the beginning of the field ramp.

An example of the spontaneous evolution to a plasma is shown in Fig. 5, in which we show the result of exciting Rb atoms to the 36*d* state and waiting 2, 5, or 12 μs before applying the field ramp. For reference, the lifetime of the Rb 36*d* state is 51 μs. The zero of the time scale is the start of the ramp. With a 2-μs delay there is a very small signal at 100 ns, from free ions collected by the beginning of the field ramp, and a large signal at 300 ns from the field ionization of the 36*d* state. Some ions are expected; they are created in several ways that we discuss shortly. What is unexpected is that with a 12-μs delay the Rydberg field ionization signal has nearly disappeared, and nearly the entire signal is contained in the early ion signal. The ion signal is so large because the cold Rydberg atoms have evolved into an ultracold plasma. That the early ion signal is a plasma is demonstrated by repeating the experiment while detecting the electrons. Figure 6 shows the result of scanning the delay between the laser pulse and the field ramp while detecting electrons ejected at the beginning of the field ramp. Truly free electrons escape, but those bound in the plasma by a few wave numbers of energy are detected. As shown by Fig. 6, no electrons are detected for 5 μs. In this short a time after the laser pulse the plasma does not form, and any free electrons simply leave the trap volume and are not detected. At longer times after the laser pulse a plasma has formed, and it traps the electrons, so they can be detected. The plasma eventually decays in tens of microseconds, as seen in the NIST experiments. Related observations of Rydberg-to-plasma evolution have been reported as well.[14,15]

That a plasma is formed seems clear enough, but to understand how it forms requires systematic measurements of the dependence of the plasma formation on the initial principal quantum number of the Rydberg atoms, the time delay after the laser pulse, and the cold-atom density. The method we use is dictated by the fact that a pulsed dye laser oscillates on random cavity modes on each laser shot, producing large fluctuations in the number of Rydberg atoms created and enormous fluctuations in the plasma signal. We set two gates, one on the Rydberg signal at 300 ns in Fig. 5, and one on the plasma signal at 100 ns in Fig. 5, and record both signals on each laser shot for fixed time delay between the laser pulse and

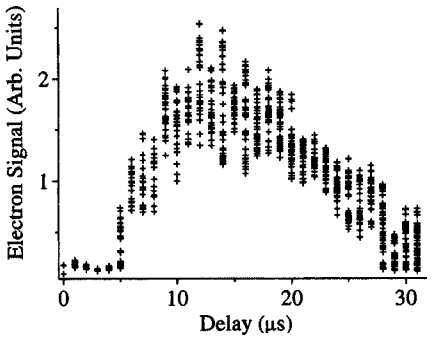

Fig. 6. Electron signal observed after excitation of the Cs 39*d* state (from Refs. 8, 12).

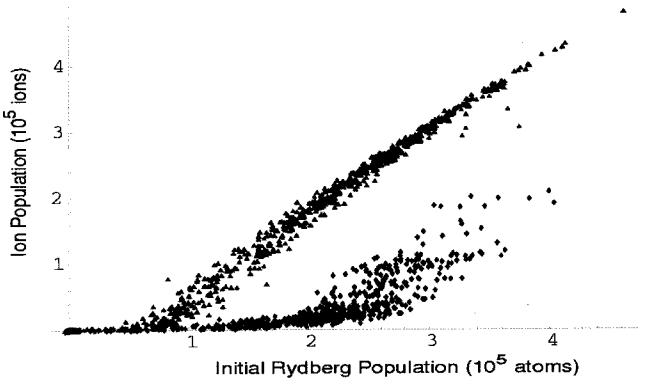

Fig. 7. Ion population as a function of initial population of the $36d$ Rydberg state for two time delays: ♦, 2 μs, the lower trace, and ▲, 12 μs, the upper trace (from Refs. 8, 11).

the field ramp. Since we do not see signals other than the plasma signal or the one from the initially excited state, we assume that the sum of these two signals is proportional to the initial Rydberg population. We sort the data into bins based on the sum of the two gated signals, i.e., the initial Rydberg population N_0, and allow the laser frequency fluctuations to vary automatically the number of Rydberg atoms created. In Fig. 7 we show the ion signal obtained versus the initial Rydberg atom number for the Rb $36d$ state and time delays of 2 and 12 μs. It is obvious that something dramatic occurs for $N_0 = 0.8 \times 10^5$ and $N_0 = 2.0 \times 10^5$ in the two data sets. However, it is more natural to think in terms of the time dependence for a fixed number of atoms. To construct a time-dependent picture, we collected data such as those shown in Fig. 7 at 100-ns delay time intervals. Taking the data from each delay for the same initial number of atoms yields the time dependence shown in Fig. 8 for two values of N_0. The number of ions initially rises slowly to a threshold value, occurring at 0.6 μs for $N_0 = 3.3 \times 10^5$ and 1.0 μs for $N_0 = 2.4 \times 10^5$. It then rises rapidly until nearly all the atoms are ionized in several microseconds. The time dependence is interpreted in the following way: The initial ionization is due to blackbody photoionization, collisions between hot (room temperature) and cold Rydberg atoms, and at high principal quantum numbers possibly overlapping or close pairs of cold Rydberg atoms. After N^+ atoms have been ionized by these processes, electrons subsequently liberated are trapped by the macroscopic positive charge. These trapped electrons pass back and forth through the cloud of Rydberg atoms, quickly ionizing them in an avalanche.

The proposed scheme is supported by more detailed investigations. Measurements were made of the initial ionization rate of the Cs $39d$ state with and without the hot Rydberg atoms from the room-temperature Cs vapor. To remove the hot atoms required turning off the trapping lasers and using one lower-power laser exactly resonant with the $6s_{1/2}$–$6p_{3/2}$ transition. With the hot atoms the ionization rate was 2000 s^{-1}; without them[8] it was 1000 s^{-1}. Calculations of the blackbody photoionization rate give 500 s^{-1} at $n = 40$,[11,16] and our estimate of the hot–cold Rydberg atom collision rate, based on the hot-atom density of 10^7 cm^{-3} and an ionization cross section 10 times the geometric cross section, as given by Olson,[17] is 1000 s^{-1}. These two rates match the observations reasonably well. For the Cs $39d$ state, when the hot atoms are removed, a plasma never forms; but for $n \geqslant 50$ a plasma forms either with or without the hot atoms. In experiments with inherently far fewer hot atoms, the plasma also forms at high n.[13] In this case some of the initial ionization may be due to close pairs of cold Rydberg atoms, much as close pairs play a central role in resonant energy transfer in a frozen Rydberg gas.[18,19]

The sudden rise in the rate of ion formation at 0.6 and 2.0 μs in Fig. 7 is due to the same electron-trapping phenomenon seen in the NIST experiment. Assuming that electrons are liberated with energies comparable with the binding energy of the initial Rydberg state, we can estimate that ~1000 ions are required to trap electrons freed later, in agreement with our observations. Further support for this notion comes from applying a small field, which inhibits the formation of a plasma. As shown by Fig. 9, a field of ~1 V/cm inhibits the formation of the plasma. Multiplying this number by the trap radius of 0.3 mm suggests that the potential well formed by the positively charged plasma is ~30 meV or 250 cm^{-1} deep, in rough agreement with the expected energies of the electrons.

We have carried out simulations of the plasma formation and compared them with our observations.[11] The essential ingredients of the model are ionization by blackbody radiation and collisions between hot and cold Rydberg atoms, with a cross section 10 times the geometric cross section. Initially only these two processes are operative. Subsequent to the creation of enough ions to trap the electrons, electron-impact ionization is added. The cross section for this process was given the value B times the geometric cross section, with B left as an adjustable parameter. In principle B should exceed 1. As shown by Fig. 10, the data and the model agree reasonably well, but B is found to be 0.2, not 1, for n from 32 to 48. That $B = 0.2$ points to the outstanding question in

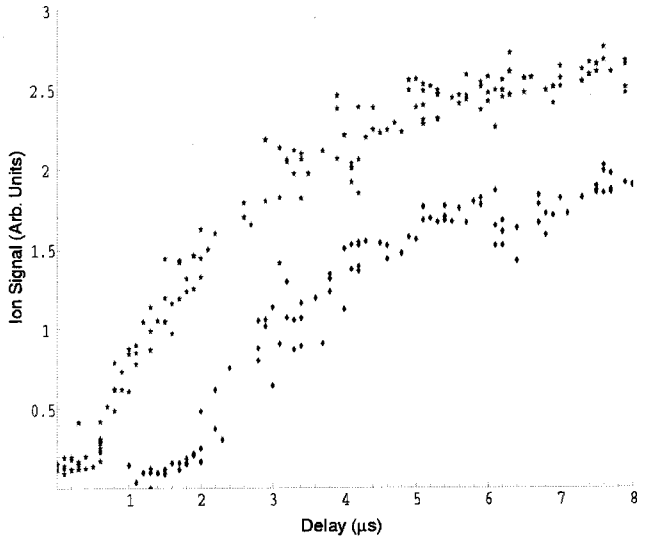

Fig. 8. Ion population as a function of interaction time for two initial populations of the $40d$ Rydberg state: ★, upper trace, 3.3×10^5 atoms, or 10.5×10^9 cm^{-3}; ♦, lower trace, 2.4×10^5 atoms or 7.6×10^9 cm^{-3}, offset by 1 μs (from Refs. 8 and 11).

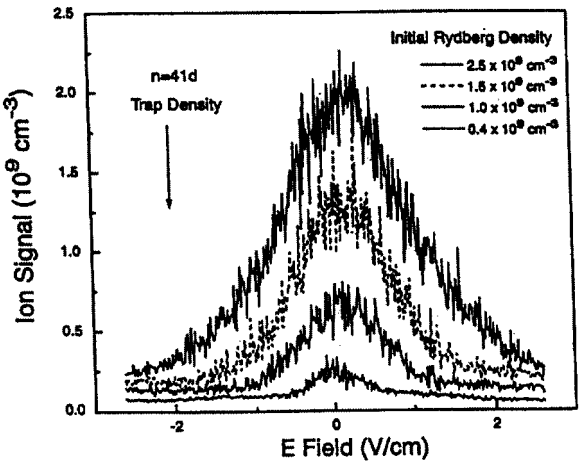

Fig. 9. Electric field dependence of the ion signal for the Rb 41*d* state; several different initial Rydberg population densities are shown for a 10-μs interaction time (from Ref. 11).

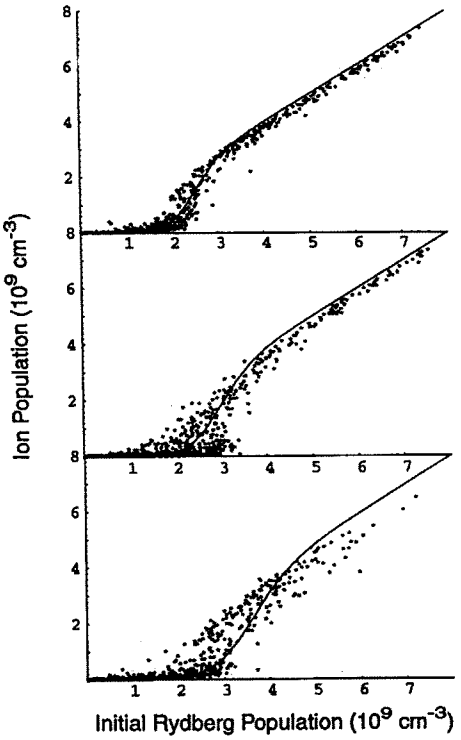

Fig. 10. Comparison between observed and simulated density dependence of the ion signal for a time delay of 10 μs for, top to bottom, Rb 44*d*, 42*d*, and 40*d* states. For all curves a 3.6% hot atom fraction is assumed, and the fit parameter B is found to be 0.244, 0.230, and 0.217, respectively (from Ref. 11).

the entire picture: What is the origin of the energy required for ionizing all the Rydberg atoms? In a plasma the electrons are essentially free, but initially they are bound by 70 cm^{-1} at $n = 40$. It is easy to identify the source of the energy in the initial ionization, but it is not yet clear what drives the ionization avalanche.

To see if adding energy hastened or enabled the formation of a plasma we have added a rf field to give the trapped electrons more energy. Specifically, we used fields at frequencies from 100 to 300 MHz. In an oscillating field $F \cos \omega t$ the average kinetic energy of a free electron, the ponderomotive energy U_p, is given by

$$U_p = \frac{1}{2} m \bar{v}^2 = \frac{F^2}{4\omega^2}. \quad (9)$$

For a 100-MHz, 1-V/cm field, $U_p = 9\ cm^{-1}$. If, when the field is applied, the electrons are already moving in the field direction with an energy of 20 cm^{-1}, they can have a peak kinetic energy of 56 cm^{-1}, which is comparable with the binding energy of an $n = 40$ atom. Consequently a 100-MHz, 1-V/cm rf field can be expected to speed the formation of a plasma if supplying the energy is normally a bottleneck. For Rydberg states of $n < 40$, adding the rf field makes a clear difference, but for states of $n > 40$ it is less clear. In general, adding energy speeds the formation of a plasma.

At this point the most likely source of the energy seems to be superelastic collisions between the trapped electrons and the cold Rydberg atoms, i.e., a mechanism proposed to heat the electrons in the NIST plasmas. However, we have seen little sign of the population of other Rydberg states by the collisions, in spite of careful searches. More refined experiments are under way to address this issue.

4. CONCLUSION

Ultracold plasmas and the related cold Rydberg gases constitute fascinating physical systems. At this moment we have what seem to be reasonable descriptions of them, but it is clear that there are aspects, such as the energy transfer processes among the electrons, both bound and free, that are not yet well understood. At the same time, it is possible to carry out experiments in which the initial conditions are well defined, and this possibility should enable us to reach a good understanding of these novel systems. For example, what happens if the initial condition is population in a single Rydberg state and a plasma of known temperature? There are also interesting future possibilities. Can the ions in the plasma be trapped optically, so the plasma does not expand? [20] Does it crystallize then? If the cold Rydberg atoms are evenly spaced, is the evolution to a plasma suppressed? Is a Mott transition then visible? Finally the issue of Rydberg-to-plasma evolution may be important for quantum information schemes.[21]

ACKNOWLEDGMENTS

This work has been supported by the U.S. Air Force Office of Scientific Research and the Centre National de la Recherche Scientifique. It is a pleasure to acknowledge stimulating discussions with R. R. Jones, J. L. Cecchi, F. Robicheaux, T. C. Killian, and S. L. Rolston and S. Mazevet.

T. F. Gallagher may be reached at tfg@virginia.edu.

REFERENCES

1. E. Nasser, *Fundamentals of Gaseous Ionization and Plasma Electronics* (Wiley, New York, 1971).

2. X. P. Huang, J. J. Bollinger, T. B. Mitchell, and W. M. Itano, "Phase-locked rotation of crystallized non-neutral plasmas by rotating electric fields," Phys. Rev. Lett. **80**, 73–76 (1998).
3. T. C. Killian, S. Kulin, S. D. Bergeson, L. A. Orozco, C. Orzel, and S. L. Rolston, "Creation of an ultracold neutral plasma," Phys. Rev. Lett. **83**, 4776–4779 (1999).
4. S. Kulin, T. C. Killian, S. D. Bergeson, and S. L. Rolston, "Plasma oscillations and expansion of an ultracold neutral plasma," Phys. Rev. Lett. **85**, 318–321 (2000).
5. T. C. Killian, M. J. Lim, S. Kulin, R. Dumke, S. D. Bergeson, and S. L. Rolston, "Formation of Rydberg atoms in an expanding ultracold neutral plasma," Phys. Rev. Lett. **86**, 3759–3762 (2001).
6. S. Mazevet, L. A. Collins, and J. D. Kress, "Evolution of ultracold neutral plasmas," Phys. Rev. Lett. **88**, 055001 (2002).
7. F. Robicheaux and J. D. Hanson, "Simulation of the expansion of an ultracold plasma," Phys. Rev. Lett. **88**, 055002 (2002).
8. M. P. Robinson, B. Laburthe-Tolra, M. W. Noel, T. F. Gallagher, and P. Pillet, "Spontaneous evolution of Rydberg atoms into an ultracold plasma," Phys. Rev. Lett. **85**, 4466–4469 (2000).
9. G. Vitrant, J. M. Raimond, M. Gross, and S. Haroche, "Rydberg to plasma evolution in a dense gas of very excited atoms," J. Phys. B **15**, L49–L55 (1982).
10. R. R. Jones, Department of Physics, University of Virginia, Charlottesville, Virginia 22904 (personal communication, 2001).
11. M. P. Robinson, "Interactions in a frozen Rydberg gas," Ph.D. thesis (University of Virginia, Charlottesville, Virginia, 2002).
12. B. Laburthe-Tolra, "Atomes, molécules et plasmas ultra-froids: transition d'un gaz de Rydberg gelé vers un plasma ultra-froid.—Contrôle de collisions de photo association dans des schémas de resonance de Feshbach et de transition Raman stimulée," Ph.D. thesis (Universite Paris-Sud, Paris, France, 2001).
13. T. F. Gallagher, *Rydberg Atoms* (Cambridge University, Cambridge, UK, 1994).
14. S. K. Dutta, D. Feldbaum, A. Walz-Flannigan, J. R. Guest, and G. Raithel, "High angular momentum states in cold Rydberg gases," Phys. Rev. Lett. **86**, 3993–3996 (2001).
15. A. Estrin, D. Tong, J. R. Ensher, C. H. Cheng, E. E. Eyler, and P. L. Gould, "Plasma formation followed by recombination in a gas of ultracold Rydberg atoms," Bull. Am. Phys. Soc. **46**, 46–47 (2001).
16. W. P. Spencer, A. G. Vaidyanathan, D. Kleppner, and T. W. Ducas, "Temperature dependence of blackbody-radiation-induced transfer among highly excited states of sodium," Phys. Rev. A **25**, 380–384 (1982).
17. R. E. Olson, "Ionization cross sections for Rydberg atom–Rydberg atom collisions," Phys. Rev. Lett. **43**, 126–129 (1979).
18. I. Mourachko, D. Comparat, F. deTomasi, A. Fioretti, P. Nosbaum, V. M. Akulin, and P. Pillet, "Many-body effects in a frozen Rydberg gas," Phys. Rev. Lett. **80**, 253–256 (1998).
19. W. R. Anderson, J. R. Veale, and T. F. Gallagher, "Resonant dipole–dipole energy transfer in a nearly frozen Rydberg gas," Phys. Rev. Lett. **80**, 249–253 (1998).
20. T. C. Killian, Department of Physics and Astronomy, Rice University, Houston, Texas 77005 (personal communication, 2001).
21. M. D. Lukin, M. Fleischauer, R. Cote, L. M. Duan, D. Jaksch, J. J. Cirac, and P. Zoller, "Dipole blockade and quantum information processing in mesoscopic atomic ensembles," Phys. Rev. Lett. **87**, 037901 (2001).